CRYSTAL GROWTH & DESIGN

pubs.acs.org/crystal

Article

Covalently Bound Gold Nanoparticle-Assisted Epitaxial Growth of Silicon Nanowires

Han Ju Lee,[‖] Chul Soon Park,[‖] Yi-Seul Park,[‖] Rami Aboumourad, Maria D. Marquez, Jin Seok Lee,* and T. Randall Lee*

Cite This: *Cryst. Growth Des.* 2020, 20, 5551−5556

Read Online

ACCESS | Metrics & More | Article Recommendations | Supporting Information

ABSTRACT: Epitaxial growth of one-dimensional nanowires has received considerable attention for vertically aligned nanoelectronic devices; however, high integration and reproducibility are still significant problems that need to be addressed. Herein, we investigated the epitaxial growth of silicon nanowires (SiNWs) using covalently bound gold nanoparticles (AuNPs) as catalysts to enhance the lattice matching between the SiNWs and the substrate. We prepared three types of alkene-terminated AuNPs for the formation of covalent bonds between the AuNPs and Si(111) substrates by ligand exchange using alkene-terminated alkanethiols with monodentate ligands (17-octadecenethiol **OET** and ((4-(undec-10-en-1-yloxy)phenyl)methanethiol **UEPMT**) and a bidentate ligand (5-(undec-10-en-1-yloxy)-1,3-phenylene)dimethanethiol **UEPDT**); the immobilization of the AuNPs was achieved by UV irradiation. Finally, we demonstrated a narrow diameter distribution and vertical alignment for the SiNWs covalently bound to the AuNPs in the assisted epitaxial growth and proposed a growth mechanism for the SiNWs using our alkene-terminated AuNPs.

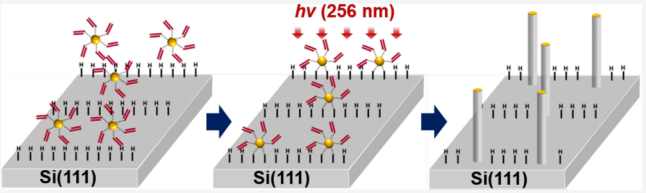

INTRODUCTION

Silicon nanowires (SiNWs) have been recognized as fundamental building blocks for emerging nanoscale devices, such as transistors,[1,2] chemical sensors,[3,4] light-emitting devices,[5,6] and solar cells,[7,8] due to their unique properties, which include their single crystal nature, mechanical flexibility, and high surface area. However, for their widespread use in the aforementioned applications, control of their alignment,[9] diameter,[10,11] and density[12,13] stand as perhaps the most challenging factors. SiNWs have been prepared by using a variety of techniques, including by means of laser ablation,[14] the supercritical fluid solution phase,[15] and chemical vapor deposition (CVD).[16] From a top-down strategy, well-defined and vertically aligned SiNWs can be prepared via lithographic patterning with anisotropic etching.[17] However, anisotropic etching induces defects, such as rough surfaces on the SiNWs sidewalls.[18] Alternatively, the vapor−liquid−solid (VLS) method allows for the growth of high quality, single-crystalline SiNWs by using a bottom-up approach, and allows for the control of key parameters such as the diameter,[19] length,[20] density,[16] and direction.[21] Single-crystalline SiNWs can also be synthesized by CVD in which growth follows the VLS growth mechanism with the assistance of a metal catalyst.[22] The diameter and position of the SiNWs following this method are mainly determined by the size and position of the metal catalyst.[23,24] Vertical growth of the SiNWs is achieved by maintaining epitaxial interfaces between the nanowires and Si substrate.

Gold nanoparticles (AuNPs) are well-known materials whose moderate chemical reactivity and solubility allow for ready use as catalysts for a wide range of catalytic reactions.[25,26] Both Au films and AuNPs have been used to catalyze the synthesis of SiNWs.[27,28] Although the epitaxial growth of SiNWs from Au films deposited on Si substrates can be easily performed, the resultant SiNWs often suffer from a broad diameter distribution.[28] In the case of SiNWs grown with citrate−AuNP catalysts, the SiNWs exhibit a narrow diameter distribution, but the epitaxial growth can suffer due to the migration of AuNPs at the temperature used to grow the nanowires.[29] For example, Hochhaum et al. used citrate-stabilized AuNPs to generate vertically aligned SiNWs via chemical vapor deposition (CVD), with $SiCl_4$ as the precursor gas and citrate-stabilized AuNPs as the catalyst on a silicon surface.[27] However, citrate-stabilized AuNPs bear a negative surface charge and cannot be evenly dispersed onto the hydrophobic silicon surface. This mismatch can lead to the migration of the particles on the surface during the growth of the SiNWs. Consequently, to overcome this shortcoming, Hochhaum et al. deposited a positively charged poly-L-lysine

Received: May 26, 2020
Revised: July 10, 2020
Published: July 10, 2020

https://dx.doi.org/10.1021/acs.cgd.0c00718
Cryst. Growth Des. 2020, 20, 5551−5556

layer to immobilize the citrate-stabilized AuNPs and inhibit their migration on the Si wafer. On the basis of their approach, the diameter distribution can be approximately controlled by the size of the citrate-stabilized AuNPs used to seed their growth.[27] Additionally, the density of the SiNWs can be controlled by adjusting the density of Au NP seeds on the surface,[12,13,16,19] which can be tuned by adjusting the concentration of AuNPs dispersed in solution.[16]

In our report, to prevent the migration of AuNPs during SiNW growth, we synthesized the alkene-terminated adsorbates shown in Figure 1 (**OET**, **UEPMT**, and **UEPDT**) and

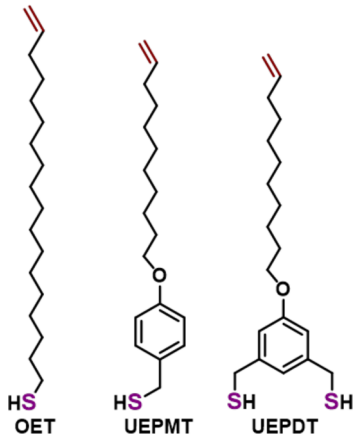

Figure 1. Alkene-terminated alkanethiols used to functionalize the Au nanoparticles: 17-octadecenethiol (**OET**), (4-(undec-10-en-1-yloxy)-phenyl)methanethiol (**UEPMT**) , and (5-(undec-10-en-1-yloxy)-1,3-phenylene)dimethanethiol (**UEPDT**).

performed ligand exchange on citrate-stabilized AuNPs to covalently immobilize the AuNPs on the Si surfaces. For these experiments, **OET** serves as a reference adsorbate that is anticipated to exhibit nanoparticle stability characteristics similar to octadecanethiol (**C18SH**). The adsorbate **UEPMT** includes an aromatic moiety that can reduce alkyl chain packing around the NP but does not include chelate stabilization. Finally, **UEPDT** features all of the possible stability-enhancing qualities used in this series of adsorbates, with the additional feature of a bidentate headgroup that has been shown to enhance colloidal stability via the "chelate effect" commonly utilized in organometallic chemistry.[30] Our approach provides two notable advantages for the growth of SiNWs on Si substrates. First, the AuNPs can be directly dispersed onto the silicon substrate without the need for any surface pretreatment, such as the deposition of a positively charged polyelectrolyte layer (poly-L-lysine).[27] Second, the covalent bonds between the alkene-functionalized AuNPs and the silicon substrate preclude the migration of the AuNPs during SiNWs growth.

EXPERIMENTAL SECTION

Materials. Undec-10-en-1-ol, octadec-17-en-1-ol, lithium aluminum hydride ($LiAlH_4$), dimethyl 5-hydroxyisophthalate, 4-(hydroxymethyl)phenol, potassium carbonate (K_2CO_3), methanesulfonyl chloride (MsCl), triethylamine (Et_3N), potassium thioacetate, and octadecanethiol (**C18SH**) were purchased from Sigma-Aldrich and used as-received. Tetrahydrofuran (THF), methanol (MeOH), dichloromethane (CH_2Cl_2), toluene, and chloroform ($CHCl_3$) were purchased from Sigma-Aldrich. Hexanes, ethyl acetate (EtOAc), and acetone were purchased from Mallinckrodt Chemicals. Anhydrous ethanol (EtOH) was purchased from Decon Lab, Inc. Distilling over calcium hydride gave dry tetrahydrofuran and dichloromethane. The silica gel for column chromatography was obtained from Sorbent Technologies. The syntheses of **OET**, **UEPMT**, and **UEPDT** are detailed in the Supporting Information.

Synthesis of Gold Nanoparticles (AuNPs). The citrate-stabilized AuNPs were obtained by the reduction of $HAuCl_4$ with trisodium citrate according to a procedure found in the literature.[31]

Preparation of Alkene-Functionalized AuNPs via Ligand Exchange. We prepared the alkene-functionalized AuNPs based on a procedure from the literature.[30] The process involves ligand exchange between the alkene-terminated alkanethiols and the initially adsorbed citrate molecules. Briefly, a suspension of AuNPs (30 nm) in 5 mL of deionized (DI) water were purged of oxygen by bubbling nitrogen gas through the suspension for 30 min. This step was followed by the injection of a THF solution of the appropriate alkene-terminated alkanethiol (6 mM, 10 mL) into the vials containing the AuNP suspensions. The final mixture was stirred for 48 h under nitrogen. The alkene-functionalized AuNPs were extracted from the mixture with toluene. The toluene-dispersed AuNPs were used to fabricate silicon nanowires without additional washing.

Stability Analysis of Alkene-Functionalized AuNPs by UV–visible Spectroscopy. The extinction spectra of the initial AuNP solution, the adsorbate-capped AuNP solutions, and the AuNP samples during the stability tests were measured at room temperature using a Cary 50 Scan UV–visible (UV–vis) optical spectrometer (Varian) operated with Cary Win UV software. The spectra of the citrate-stabilized AuNPs were collected in an aqueous solution in a quartz cuvette having a 1 cm optical path length, scanning over a range of wavelengths (400–800 nm). The spectra of the adsorbate-capped AuNPs were collected in 1:1 toluene/THF solutions. The colloidal stability of AuNPs can be estimated by UV–vis spectroscopy, as shown in previous reports.[32] For such studies, the particle size, stabilizer, and surrounding medium each have an influence on the surface plasmon resonance (SPR) of the Au nanoparticles.[33] Furthermore, if the AuNPs aggregate and sink to the bottom of the cuvette, red shifting, broadening, and lowering of the SPR bands will be observed.[33]

Alkene-Functionalized AuNPs Covalently Bound on Si(111) Substrates. A Si(111) substrate with dimensions of 0.5 cm (width) × 5 cm (length), which was obtained from LG siltron, was rinsed with water and buffered HF solution (Acros). A solution containing the 30 nm alkene-terminated AuNPs (toluene:THF = 1:1) was dropped onto the surface of the as-prepared Si(111) substrate and dried using nitrogen gas. Then, the Au-covered Si substrate was loaded into the center of 1 in. quartz tube, and the quartz tube was evacuated and flushed repeatedly with H_2 gas to minimize oxygen gas. In order to chemically bind the AuNPs to the Si(111) substrate, the Au-covered Si substrate was irradiated with ultraviolet light (254 nm) for 1 h by UV lamp. After irradiation, the prepared Si substrate was sonicated in toluene solution to remove any AuNPs that were physisorbed to the substrate.

Citrate-Stabilized AuNP-Dispersed Si(111) Substrates. A Si(111) substrate with dimensions of 0.5 cm (width) × 5 cm (length) was rinsed with water and buffered HF solution. Then, the Si substrate was dipped for 3 min into an aqueous poly-L-lysine solution (0.1% w/v, Ted Pella). A solution containing the 30 nm citrate-stabilized AuNPs was dropped onto the surface of the as-prepared Si(111) substrate and dried using a stream of nitrogen gas. Without additional treatments (e.g., baking), the citrate-capped AuNP-dispersed Si samples were used for the growth of SiNWs.

Preparation of 1 Nanometer-Thick Au-Nanofilm Substrates. The methods used here have been described previously;[34] additional experimental details are provided in the following. The Si(111) wafer was first cleaned with acetone and isopropyl alcohol and then dried using a stream of nitrogen gas. The substrate was subsequently dipped for 4 min into a buffered HF solution (9% of a 48–52% HF solution in water, 32% of a ~40% NH_4F solution in water) to remove the native oxide layer. The substrate was then rinsed with water. The as-prepared Si(111) wafer was then covered with a 1 nm-thick Au film

https://dx.doi.org/10.1021/acs.cgd.0c00718
Cryst. Growth Des. 2020, 20, 5551–5556

by e-beam evaporation. Next, the substrate was diced into small pieces with dimensions of 0.5 cm (width) × 5 cm (length), with each resulting Au-covered substrate being used for SiNW growth.

Growth of Silicon Nanowires. SiNWs were synthesized by CVD using $SiCl_4$ (Sigma-Aldrich) as the Si precursor, 10% H_2 in Ar as the carrier gas and dilution gas, and the respective gold samples as the catalyst (**UEPDT**-capped AuNPs, citrate-stabilized AuNPs, and the 1 nm-thick Au nanofilms, AuNFs). Prior to the experiment, the quartz tube was evacuated and flushed repeatedly with 10% H_2 gas (high purity, 99.999%) to minimize oxygen contamination. Then, the Au-covered Si substrate was loaded into the center of a 1 in. diameter quartz tube furnace, and the substrate was heated to a growth temperature of 860 °C with a rate of 20 °C/min. When the temperature reached the growth temperature, SiNWs were synthesized for 10 min. In the case of SiNWs grown from alkene-terminated AuNPs and citrate-terminated AuNPs, the carrier and dilution gases were introduced at flow rates of 60 and 300 sccm, respectively. For the growth of SiNWs using the AuNF, the carrier and dilution gases were introduced at flow rates of 100 and 750 sccm, respectively. After 10 min of NW growth, the supply of Si precursor was stopped, and the reactor was cooled to room temperature. See Scheme 1 for an illustration of SiNW growth by covalent immobilization.

Characterization of Silicon Nanowires. SiNWs were characterized by scanning electron microscopy (SEM) (JEOL JSM-7600F) at an acceleration voltage of 15 kV. X-ray diffraction (XRD) patterns of the SiNWs were obtained using a Rigaku diffractometer (D/MAX-1C).

Scheme 1. Illustration of Silicon Nanowire Growth by Covalent Immobilization of Alkene-Functionalized Gold Nanoparticles

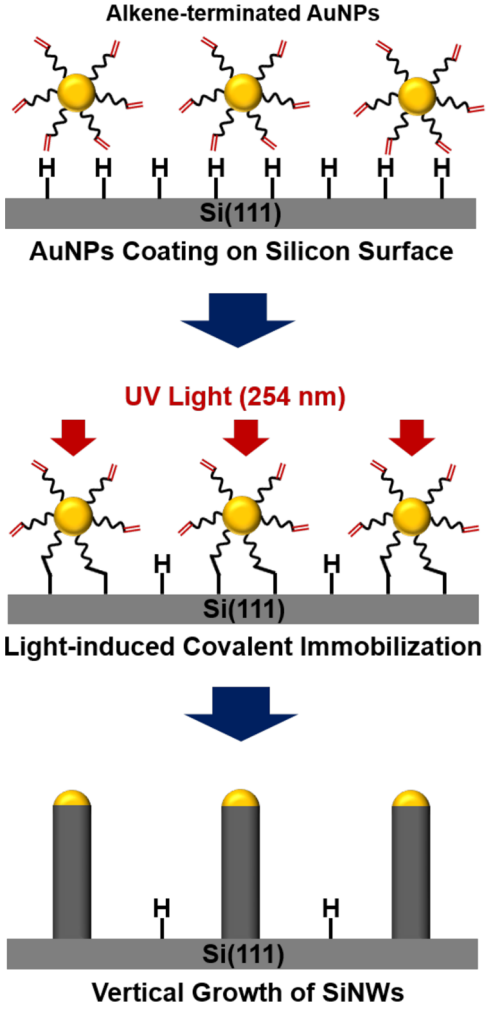

RESULTS AND DISCUSSION

Colloidal Stability of the Functionalized AuNPs. After ligand exchange, the colloidal stability of the AuNPs capped with **C18SH**, **OET**, **UEPMT**, and **UEPDT** were evaluated since the colloidal stability of protected AuNPs highly influences the distribution of the AuNPs on the Si(111) surface.[27] Optical images of the protected AuNP solutions are shown in Figure 2. According to the images, the AuNPs

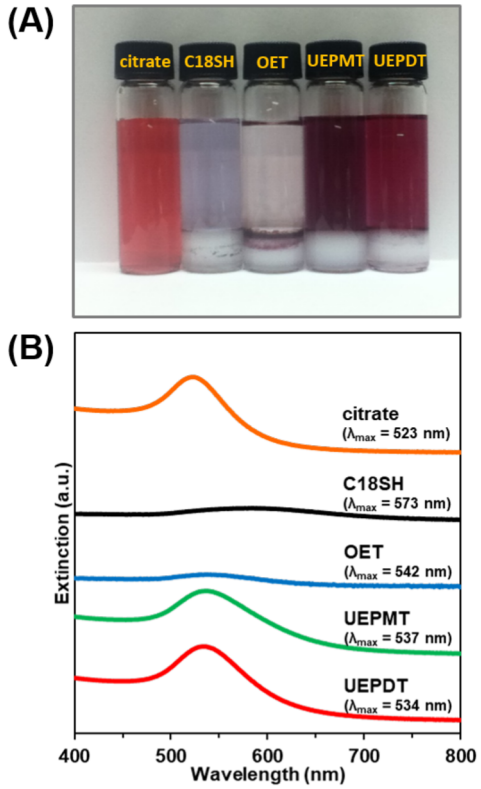

Figure 2. (A) Optical images and (B) visible spectra of 30 nm AuNPs capped with citrate, **C18SH**, **OET**, **UEPMT**, and **UEPDT** after phase transfer into 1:1 toluene/THF solutions. The citrate-stabilized AuNPs in DI water are shown as a reference.

capped with **C18SH** and **OET** were the least stable and exhibited complete precipitation as well as loss of color in the solution, as shown in Figure 2A. On the other hand, the AuNPs protected with **UEPMT** and **UEPDT** exhibited no significant color changes in the organic solution, as presented in Figure 2A. Visually, the AuNPs capped with **UEPDT** exhibited the greatest colloidal stability, as indicated by the slight change in the solution color to purplish (consistent with a small amount of aggregation present in the organic solution). The images allow for a visual means of determining the relative colloidal stability of the functionalized AuNPs, which in this study is as follows: **UEPDT** > **UEPMT** > **OET** = **C18SH**.

More precisely, the colloidal stability of functionalized AuNPs dispersed in a solvent can be characterized by UV−vis spectroscopy.[29] Specifically, the surface plasmon resonance (SPR) bands of AuNPs are highly influenced by the particle size, protectant, and surrounding medium.[35] Furthermore, the aggregation of the AuNPs, which commonly leads to

https://dx.doi.org/10.1021/acs.cgd.0c00718
Cryst. Growth Des. 2020, 20, 5551−5556

precipitation, also leads to red shifts, peak broadening, and a reduced intensity of the SPR bands.[35] To compare the colloidal stability in organic solution of the AuNPs capped with each of the adsorbates, we measured the extinction spectra for each of the AuNPs capped with **C18SH**, **OET**, **UEPMT**, and **UEPDT** as well as the citrate-stabilized AuNPs as a control sample. As presented in Figure 2B, the ∼30 nm citrate-stabilized AuNPs exhibited a λ_{max} at 523 nm. However, the AuNPs protected with **C18SH** and **OET** exhibited remarkable red shifts to 573 and 542 nm, respectively. Separately, the AuNPs coated with **UEPMT** and **UEPDT** showed a smaller red shift at 537 and 534 nm, respectively. From these results, we can conclude that the AuNPs coated with the bidentate adsorbate (**UEPDT**) exhibited the greatest colloidal stability and confirm that the relative colloidal stability of the AuNPs functionalized with the adsorbates is as follows: **UEPDT** > **UEPMT** ≫ **OET** = **C18SH**. The greater stability of the **UEPDT**-coated AuNPs compared to the other coated AuNPs can be attributed to the chelate effect afforded by the bidentate nature of the adsorbate.[30] The chelating adsorbate disfavors the formation of intramolecular disulfides as well as intermolecular oligomeric disulfides.[30]

Growth of SiNWs. Upon the basis of the greater colloidal stability of the **UEPDT**-capped AuNPs compared to the other adsorbates, the **UEPDT**-capped AuNPs were used to grow SiNWs. The performance of the **UEPDT**-capped AuNPs were evaluated and compared to traditionally employed Au catalysts, citrate-stabilized AuNPs, and 1 nm-thick gold nanofilm (AuNF). The **UEPDT**-capped AuNPs were immobilized via UV irradiation to bind the alkene termini of the adsorbates covalently to the Si(111) surface. To verify the covalent immobilization of the **UEPDT**-capped AuNPs to the Si(111) surface after UV irradiation, the **UEPDT**−AuNPs were distributed on Si(111) surfaces without UV irradiation and sonicated for 5s. Afterward, we attempted to grow SiNWs on these surfaces and failed to observe the epitaxial SiNWs on the surface, as shown in Figure 3. Failure to observe the SiNWs on

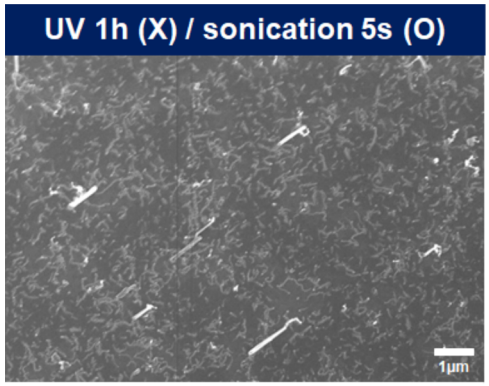

Figure 3. Tilt-view SEM image at 20° of the SiNWs synthesized using **UEPDT**-capped AuNPs without UV irradiation.

the surface was likely due to the removal of **UEPDT**-capped AuNPs during the sonication procedure, highlighting the imperative role the covalent bonding between the **UEPDT**-capped AuNPs and the Si(111) surface after UV irradiation plays for the growth of epitaxial SiNWs.

The grown SiNWs with UV irradiation were characterized by SEM and X-ray diffraction patterns. Figure 4 shows 20° tilt-view SEM images, the diameter distribution, and X-ray diffraction (XRD) patterns of the synthesized SiNWs using the three Au catalysts: (1) citrate-stabilized AuNPs, (2) 1 nm-thick AuNF, (3) **UEPDT**-capped AuNPs. The diameter distribution of the SiNWs is predominantly influenced by the size and distribution of the Au catalyst and is imperative to maintaining epitaxial interfaces between the SiNWs and the Si substrate to achieve vertical growth. As presented in Figure 4A (c) and Figure 4B (c), the SiNWs grown from the **UEPDT**-capped AuNPs exhibited a narrower diameter distribution compared to the other Au catalysts (citrate-stabilized AuNPs (see Figure 4A (a)) and AuNF (see Figure 4B (b)) and arises from the covalent bond between the alkene termini of the **UEPDT**-capped AuNPs and the Si(111) surface after UV irradiation. Furthermore, the covalent bonding precludes the migration of the AuNPs on the surfaces at the SiNWs growth temperature. Additionally, the covalent bond between the **UEPDT**-capped AuNPs and the Si(111) surface maintains epitaxial interfaces between the SiNWs and the Si substrate.

In contrast, the SiNWs grown with the citrate-stabilized AuNPs electrostatically immobilized on the positively charged polyelectrolyte layer (poly-L-lysine) exhibited a broader diameter distribution, as shown in Figure 4A (a) and Figure 4B (a), likely caused by the agglomeration of the particles as a consequence of their migration on the Si(111) surface at the growth temperature. Furthermore, the increase in temperature of the substrate during the growth of the SiNWs induced cracking and migration of the AuNFs, giving rise to liquid-like Au nanodroplets of various sizes; the latter allows for agglomeration into larger particles by van der Waals attractive forces, Ostwald ripening, and coalescence.[36,37] Due to the aforementioned reason, the SiNWs grown from the AuNFs exhibited the broadest diameter distribution, as shown in Figure 4B (b). On the basis of our results, the diameter distribution of the SiNWs grown from different Au catalysts follows the trend: **UEPDT**-capped AuNPs < citrate-stabilized AuNPs < AuNFs (see Figure 4B). More importantly, our results confirm that our strategy of using a covalently bonded Au catalyst allows for the successful growth of epitaxial SiNWs with a narrow diameter distribution.

Additionally, Figure 4C (a), (b), and (c) show the X-ray diffraction (XRD) of the SiNWs grown from the citrate-stabilized AuNPs, 1 nm-thick AuNFs, and **UEPDT**-capped AuNPs, respectively. All samples exhibited a major peak at 28.58° on the XRD patterns corresponding to the (111) direction. Unlike the SiNWs grown from the AuNFs (see Figure 4C (b)), no minor peaks are discernible at 47.56 or 56.40° corresponding to the (220) and (311) directions for the SiNWs grown with the citrate-stabilized AuNPs and the **UEPDT**-capped AuNPs (see Figure 4C (a) and (c), respectively), indicating that the growth of the SiNWs from the AuNPs is restricted to the (111) direction.

■ CONCLUSIONS

The vertically aligned SiNWs were obtained by covalently immobilizing AuNPs functionalized with alkene-terminated SAMs using UV irradiation. The covalently immobilized AuNPs prevent the migration/agglomeration of the AuNPs on the Si(111) substrate and allow for the growth of vertically aligned SiNWs. Covalent bonding was achieved between the alkene termini of **UEPDT**-capped AuNPs and the substrate by UV irradiation, producing well-defined and vertically aligned epitaxial SiNWs on Si(111) surfaces. On the basis of our findings, we believe the strategy presented herein can improve

https://dx.doi.org/10.1021/acs.cgd.0c00718
Cryst. Growth Des. 2020, 20, 5551−5556

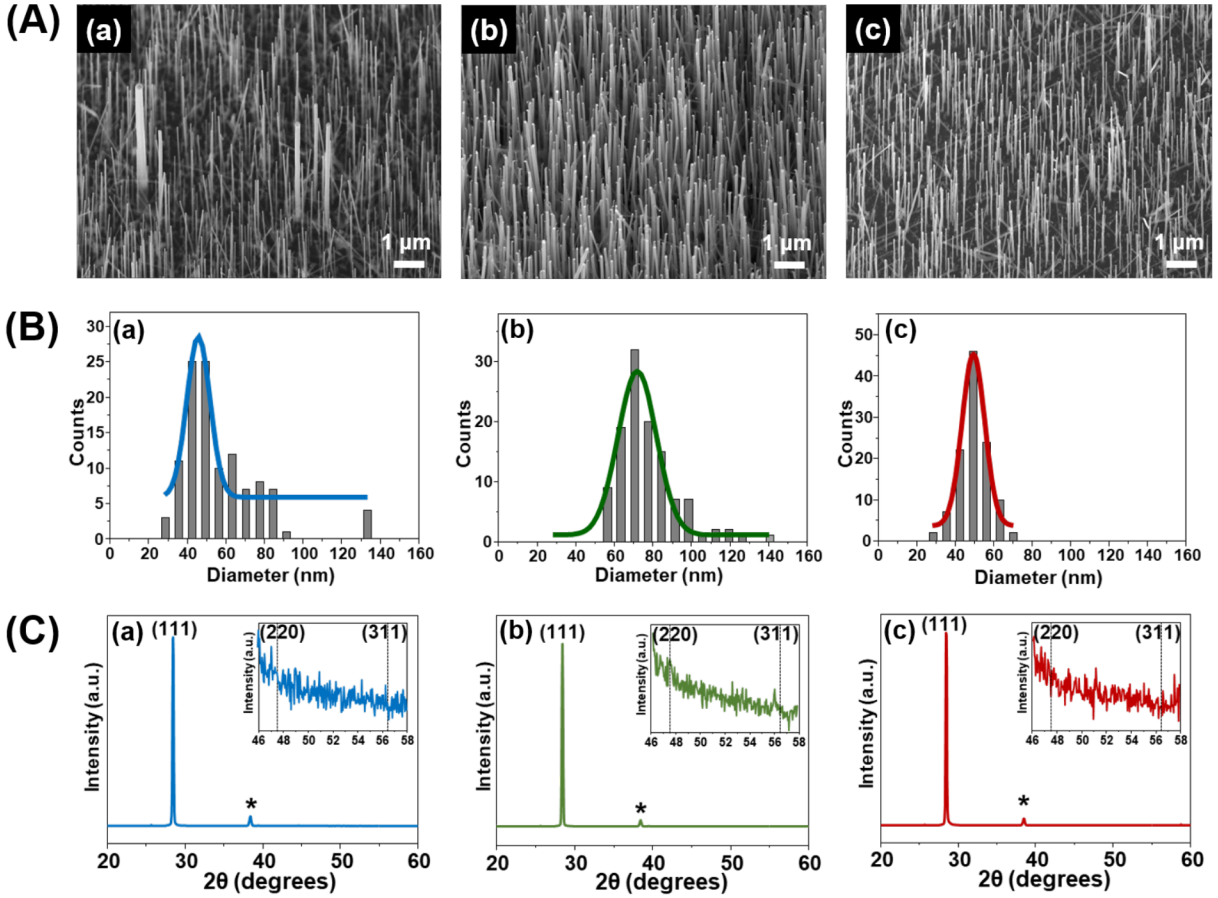

Figure 4. A (a–c) 20° tilt-view SEM images, B (a–c) diameter distributions, and C (a–c) X-ray diffraction (XRD) of SiNWs synthesized from citrate-stabilized AuNPs, 1 nm-thick AuNF, **UEPDT**-capped AuNPs, respectively. The XRD peak marked with an asterisk arises from the Au present at the tip of the SiNWs.

nanowire-based engineering to precisely control the diameter, alignment, and density of SiNWs on Si(111) surfaces. By altering the size and concentration of the alkene-terminated AuNPs, parameters such as the diameter/alignment of the SiNWs and their density on Si(111) surfaces can be precisely controlled. Finally, our strategy can also provide greater insight into the epitaxial growth of one-dimensional nanostructures, such as the patterned growth of SiNWs, for use in next-generation electronic devices.

■ ASSOCIATED CONTENT

Supporting Information

The Supporting Information is available free of charge at https://pubs.acs.org/doi/10.1021/acs.cgd.0c00718.

Descriptions of the synthetic procedures for **OET**, **UEPMT**, and **UEPDT**, including characterization data (^{1}H and ^{13}C NMR spectra) for **UEPMT** and **UEPDT** (PDF)

■ AUTHOR INFORMATION

Corresponding Authors

T. Randall Lee − *Department of Chemistry and the Texas Center for Superconductivity, University of Houston, Houston, Texas 77204-5003, United States;* orcid.org/0000-0001-9584-8861; Email: trlee@uh.edu

Jin Seok Lee − *Department of Chemistry, Hanyang University, Seoul 04763, Korea*; Email: jseoklee@hanyang.ac.kr

Authors

Han Ju Lee − *Department of Chemistry and the Texas Center for Superconductivity, University of Houston, Houston, Texas 77204-5003, United States*

Chul Soon Park − *Department of Chemistry and the Texas Center for Superconductivity, University of Houston, Houston, Texas 77204-5003, United States*

Yi-Seul Park − *Materials and Life Science Research Division, Korea Institute of Science and Technology, Seoul 02792, Korea*

Rami Aboumourad − *Department of Chemistry and the Texas Center for Superconductivity, University of Houston, Houston, Texas 77204-5003, United States*

Maria D. Marquez − *Department of Chemistry and the Texas Center for Superconductivity, University of Houston, Houston, Texas 77204-5003, United States*

Complete contact information is available at: https://pubs.acs.org/10.1021/acs.cgd.0c00718

Author Contributions

‖These authors contributed equally.

Notes

The authors declare no competing financial interest.

■ ACKNOWLEDGMENTS

We thank the National Science Foundation (CHE-1710561), the Robert A. Welch Foundation (Grant No. E-1320), and the Texas Center for Superconductivity at the University of

https://dx.doi.org/10.1021/acs.cgd.0c00718
Cryst. Growth Des. 2020, 20, 5551−5556

Houston for generous support. Additional support for this work was generously provided by the Basic Science Research Program through the National Research Foundation of Korea (NRF) funded by the Ministry of Science, ICT & Future Planning (2017R1E1A1A01075377).

REFERENCES

(1) Kim, H. Y.; Lee, K.; Lee, J. W.; Kim, S.; Kim, G. T.; Duesberg, G. S. Electrical Properties of High Density Arrays of Silicon Nanowire Field Effect Transistors. *J. Appl. Phys.* **2013**, *114*, 144503−1−144503−7.
(2) Masood, M. N.; Carlen, E. T.; van den Berg, A. All-(111) Surface Silicon Nanowire Field Effect Transistor Devices: Effects of Surface Preparations. *Mater. Sci. Semicond. Process.* **2014**, *27*, 758−764.
(3) Lupan, O.; Chow, L.; Pauporte, T.; Ono, L.K.; Roldan Cuenya, B.; Chai, G. Highly Sensitive and Selective Hydrogen Single-Nanowire Nanosensor. *Sens. Actuators, B* **2012**, *173*, 772−780.
(4) Talin, A. A.; Hunter, L. L.; Léonard, F.; Rokad, B. Large Area, Dense Silicon Nanowire Arrays Chemical Sensor. *Appl. Phys. Lett.* **2006**, *89*, 153102−1−153102−3.
(5) Duan, X.; Huang, Y.; Agarwal, R.; Lieber, C. M. Single-Nanowire Electrically Driven Lasers. *Nature* **2003**, *421*, 241−245.
(6) Huang, M. H.; Mao, S.; Feick, H.; Yan, H.; Wu, Y.; Kind, H.; Weber, E.; Russo, R.; Yang, P. Room-Temperature Ultraviolet Nanowire Nanolasers. *Science* **2001**, *292*, 1897−1899.
(7) Zhang, A.; You, S.; Soci, C.; Liu, Y.; Wang, D.; Lo, Y.-H. Silicon Nanowire Detectors Showing Phototransistive Gain. *Appl. Phys. Lett.* **2008**, *93*, 121110−1−121110−1.
(8) Gunawan, O.; Guha, S. Characteristics of Vapor-Liquid-Solid Grown Silicon Nanowire Solar Cells. *Sol. Energy Mater. Sol. Cells* **2009**, *93*, 1388−1393.
(9) Schmidt, V.; Senz, S.; Gösele, U. Diameter-Dependent Growth Directions of Epitaxial Silicon Nanowires. *Nano Lett.* **2005**, *5*, 931−935.
(10) Brus, L. Luminescence of Silicon Materials: Chains, Sheets, Nanocrystals, Nanowires, Microcrystals, and Porous Silicon. *J. Phys. Chem.* **1994**, *98*, 3575−3581.
(11) Seo, K.; Wober, M.; Steinvurzel, P.; Schonbrun, E.; Dan, Y.; Ellenbogen, T.; Crozier, K. B. Multicolored Vertical Silicon Nanowires. *Nano Lett.* **2011**, *11*, 1851−1856.
(12) Kendrick, C. E.; Redwing, J. M. The Effect of Pattern Density and Wire Diameter on the Growth Rate of Micron Diameter Silicon Wires. *J. Cryst. Growth* **2011**, *337*, 1−6.
(13) Bucaro, M. A.; Vasquez, Y.; Hatton, B. D.; Aizenberg, J. Fine-Tuning the Degree of Stem Cell Polarization and Alignment on Ordered Arrays of High-Aspect-Ratio Nanopillars. *ACS Nano* **2012**, *6*, 6222−6230.
(14) Morales, A. M.; Lieber, C. M. A Laser Ablation Method for the Synthesis of Crystalline Semiconductor Nanowires. *Science* **1998**, *279*, 208−211.
(15) Holmes, J. D.; Johnston, K. P.; Doty, R. C.; Korgel, B. A. Control of Thickness and Orientation of Solution-Grown Silicon Nanowires. *Science* **2000**, *287*, 1471−1473.
(16) Hochbaum, A. I.; Fan, R.; He, R.; Yang, P. Controlled Growth of Si Nanowire Arrays for Device Integration. *Nano Lett.* **2005**, *5*, 457−460.
(17) Huang, Z.; Fang, H.; Zhu, J. Fabrication of Silicon Nanowire Arrays with Controlled Diameter, Length, and Density. *Adv. Mater.* **2007**, *19*, 744−748.
(18) Chen, Y.; Xu, X.; Gartia, M. R.; Whitlock, D.; Lian, Y.; Liu, L. Ultrahigh Throughput Silicon Nanomanufacturing by Simultaneous Reactive Ion Synthesis and Etching. *ACS Nano* **2011**, *5*, 8002−8012.
(19) Cui, Y.; Lauhon, L. J.; Gudiksen, M. S.; Wang, J.; Lieber, C. M. Diameter-Controlled Synthesis of Single-Crystal Silicon Nanowires. *Appl. Phys. Lett.* **2001**, *78*, 2214−2216.
(20) Eichfeld, S. M.; Shen, H.; Eichfeld, C. M.; Mohney, S. E.; Dickey, E. C.; Redwing, J. M. Gas Phase Equilibrium Limitations on The Vapor−Liquid−Solid Growth of Epitaxial Silicon Nanowires using $SiCl_4$. *J. Mater. Res.* **2011**, *26*, 2207−2214.
(21) Ge, S.; Jiang, K.; Lu, X.; Chen, Y.; Wang, R.; Fan, S. Orientation-Controlled Growth of Single-Crystal Silicon-Nanowire Arrays. *Adv. Mater.* **2005**, *17*, 56−61.
(22) Wagner, R. S.; Ellis, W. C. Vapor-Liquid-Solid Mechanism of Single Crystal Growth. *Appl. Phys. Lett.* **1964**, *4*, 89−90.
(23) Cui, Y.; Lauhon, L. J.; Gudiksen, M. S.; Wang, J.; Lieber, C. M. Diameter-Controlled Synthesis of Single-Crystal Silicon Nanowires. *Appl. Phys. Lett.* **2001**, *78*, 2214−2216.
(24) Kayes, B. M.; Filler, M. A.; Putnam, M. C.; Kelzenberg, M. D.; Lewis, N. S.; Atwater, H. A. Growth of Vertically Aligned Si Wire Arrays over Large Areas (>1 cm^2) with Au and Cu Catalysts. *Appl. Phys. Lett.* **2007**, *91*, 103110.
(25) Hashmi, A. S. K. Gold-Catalyzed Organic Reactions. *Chem. Rev.* **2007**, *107*, 3180−3211.
(26) Daniel, M.-C.; Astruc, D. Gold Nanoparticles: Assembly, Supramolecular Chemistry, Quantum-Size-Related Properties, and Applications toward Biology, Catalysis, and Nanotechnology. *Chem. Rev.* **2004**, *104*, 293−346.
(27) Hochbaum, A. I.; Fan, R.; He, R.; Yang, P. Controlled Growth of Si Nanowire Arrays for Device Integration. *Nano Lett.* **2005**, *5*, 457−460.
(28) Wu, Y.; Yan, H.; Huang, M.; Messer, B.; Song, J.; Yang, P. Inorganic Semiconductor Nanowires: Rational Growth, Assembly, and Novel Properties. *Chem. - Eur. J.* **2002**, *8*, 1260−1268.
(29) Oh, E. K.; Susumu, K.; Mäkinen, A. J.; Deschamps, J. R.; Huston, A. L.; Medintz, I. L. Colloidal Stability of Gold Nanoparticles Coated with Multithiol-Poly(ethylene glycol) Ligands: Importance of Structural Constraints of the Sulfur Anchoring Groups. *J. Phys. Chem. C* **2013**, *117*, 18947−18956.
(30) Zhang, S.; Leem, G.; Srisombat, L.; Lee, T. R. Rationally Designed Ligands that Inhibit the Aggregation of Large Gold Nanoparticles in Solution. *J. Am. Chem. Soc.* **2008**, *130*, 113−120.
(31) Frens, G. Controlled Nucleation for the Regulation of the Particles Size in Monodisperse Gold Suspensions. *Nature, Phys. Sci.* **1973**, *241*, 20−22.
(32) Weisbecker, C. S.; Merritt, M. V.; Whitesides, G. M. Molecular Self-Assembly of Aliphatic Thiols on Gold Colloids. *Langmuir* **1996**, *12*, 3763−3772.
(33) Underwood, S.; Mulvaney, P. Effect of the Solution Refractive Index on the Color of Gold Colloids. *Langmuir* **1994**, *10*, 3427−343.
(34) Park, Y.-S.; Jung, D. H.; Kim, H. J.; Lee, J. S. Annealed Au-Assisted Epitaxial Growth of Si Nanowires: Control of Alignment and Density. *Langmuir* **2015**, *31*, 4290−4298.
(35) Wiesner, J.; Wokaun, A. Anisotropic Gold Colloid. Preparation, Characterization, and Optical Properties. *Chem. Phys. Lett.* **1989**, *157*, 569−575.
(36) De Los Santos, V. L.; Lee, D.; Seo, J.; Leon, F. L.; Bustamante, D. A.; Suzuki, S.; Majima, Y.; Mitrelias, T.; Ionescu, A.; Barnes, C. H.W. Crystallization and Surface Morphology of Au/SiO_2 Thin Films Following Furnace and Flame Annealing. *Surf. Sci.* **2009**, *603*, 2978−2985.
(37) Hannon, J. B.; Kodambaka, S.; Ross, F. M.; Tromp, R. M. The Influence of the Surface Migration of Gold on the Growth of Silicon Nanowires. *Nature* **2006**, *440*, 69−71.

https://dx.doi.org/10.1021/acs.cgd.0c00718
Cryst. Growth Des. 2020, 20, 5551−5556